Supporting Information

Tandem-like vanadium clusters chains in a polyoxovanadate-based metal–organic framework for efficiently catalytic oxidation of sulfides

Tian-Yi Dang,[a†] Run-Han Li,[a†] Hong-Rui Tian,[a] Qian Wang,[a] Ying Lu*[a] and Shu-Xia Liu*[a]

[a]*Key Laboratory of Polyoxometalate and Reticular Material Chemistry of the Ministry of Education, College of Chemistry, Northeast Normal University, Changchun, Jilin 130024, P. R. China.*

E-mail: luy968@nenu.edu.cn; liusx@nenu.edu.cn

Table of Contents

1. Crystallographic Data and Structure Refinements

Table S1. Crystallographic data and structure refinement of **V-Ni-MOF**

Name	V-Ni-MOF
Empirical formula	$C_{28}H_{28}N_8NiO_{11}V_4$
Formula weight	915.05
Temperature (K)	295.05
Wave length (Å)	0.71073
Crystal system	monoclinic
Space group	C2/c
a (Å)	24.916(2)
b (Å)	11.1241(10)
c (Å)	16.1128(13)
α (deg)	90
β (deg)	126.088(2)
γ (deg)	90
Volume ($Å^3$)	3609.1(6)
Z, Dcalc (Mg/m^3)	4, 1.684
Absorption coefficient (mm^{-1})	1.576
F (000)	1840.0
Crystal size (mm^3)	0.21 × 0.2 × 0.19
θ range (deg)	2.227 to 25.074
index range (deg)	$-29 \leq h \leq 29$, $-13 \leq k \leq 13$, $-19 \leq l \leq 18$
Reflections collected / unique	27823 / 3212 [R_{int} = 0.0777]
Data / restraints / parameters	3212 / 133 / 317
Goodness-of-fit on F^2	1.043
R1, wR_2 ($I > 2\sigma(I)$)	0.0416, 0.0970
R1, wR_2 (all data)	0.0721, 0.1142
Largest diff. peak and hole (e $Å^{-3}$)	0.40, -0.54

$R_1 = \sum||F_o|-|F_c||/\sum|F_o| \cdot wR_2 = [\sum[w(F_o^2-F_c^2)^2]/\sum[w(F_o^2)^2]]^{1/2}$

Table S2. Selected bond lengths [Å] and angles [deg] for **V-Ni-MOF**

V-Ni-MOF			
Ni(1)-O(1)[1]	2.097(3)	Ni(1)-O(1)	2.097(3)
Ni(1)-N(3)	2.072(3)	Ni(1)-N(3)[1]	2.072(3)
Ni(1)-N(1)	2.090(3)	Ni(1)-N(1)[1]	2.090(3)
V(1)-O(1)	1.602(3)	V(1)-O(2)	1.587(4)
V(1)-O(0AA)	1.783(11)	V(1)-O(4AA)	1.803(15)
V(2)-O(0AA)[3]	1.747(12)	V(2)-O(6A)	1.569(10)
V(2)-O(2AA)[2]	1.779(14)	V(2)-O(4AA)	1.798(14)
O(1)[1]-Ni(1)-O(1)	180.0	N(3)[1]-Ni(1)-N(1)[1]	85.88(11)
N(3)[1]-Ni(1)-N(1)	94.13(11)	N(3)-Ni(1)-O(1)	90.47(11)
N(3)-Ni(1)-O(1)[1]	89.53(11)	N(3)[1]-Ni(1)-N(3)	180
N(1)[1]-Ni(1)-N(1)	180	O(1)-Ni(1)-N(1)	89.52(12)
O(1)-Ni(1)-N(1)[1]	90.48(12)	O(0AA)-V(1)-O(1)	120.4(4)
O(0AA)-V(1)-O(2)	93.3(4)	O(4AA)-V(1)-O(2)	99.2(4)
O(4AA)-V(1)-O(1)	114.1(5)	O(2)-V(1)-O(1)	109.3(2)
O(6A)-V(2)-O(2AA)[2]	110.7(5)	O(6A)-V(2)-O(0AA)[3]	112.6(6)
O(0AA)[3]-V(2)-O(2AA)[2]	103.8(5)		

[1] 1-X,1-Y,1-Z; [2] 1-X,+Y,1/2-Z; [3] 1-X,2-Y,1-Z.

2. The asymmetric unit of V-Ni-MOF

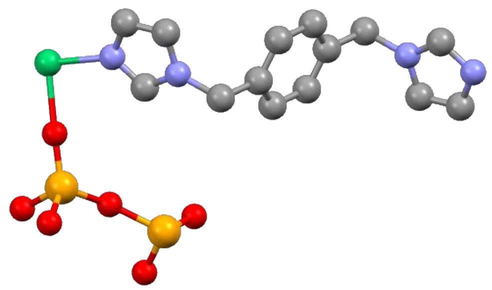

Figure S1. The asymmetric unit of **V-Ni-MOF**.

3. PXRD patterns of V-Ni-MOF

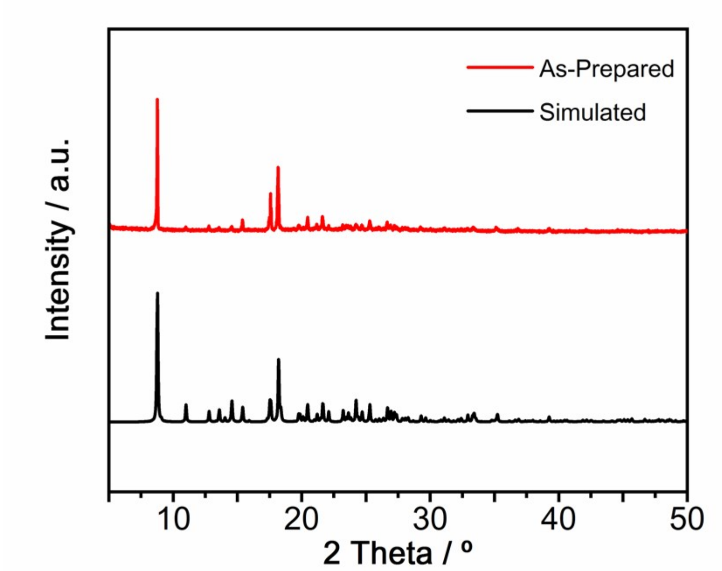

Figure S2. The PXRD patterns of **V-Ni-MOF**.

4. FTIR Spectrum of V-Ni-MOF

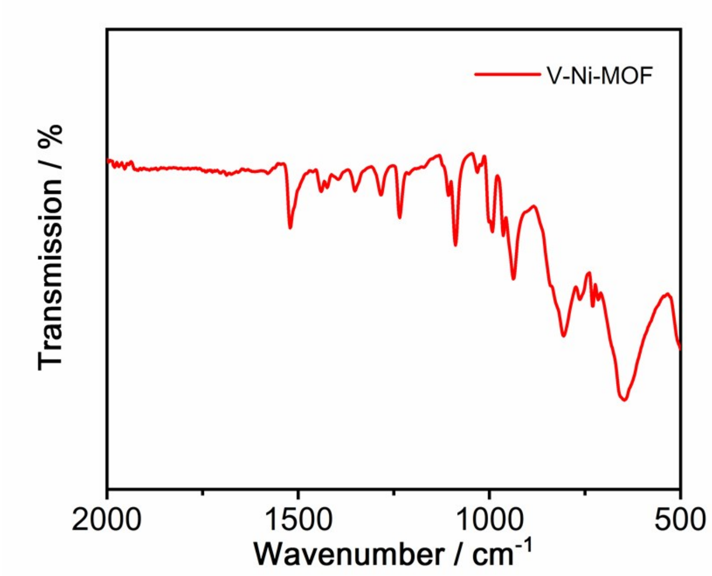

Figure S3. The FTIR spectrum of **V-Ni-MOF**.

5. XPS Spectra of V and Ni in V-Ni-MOF

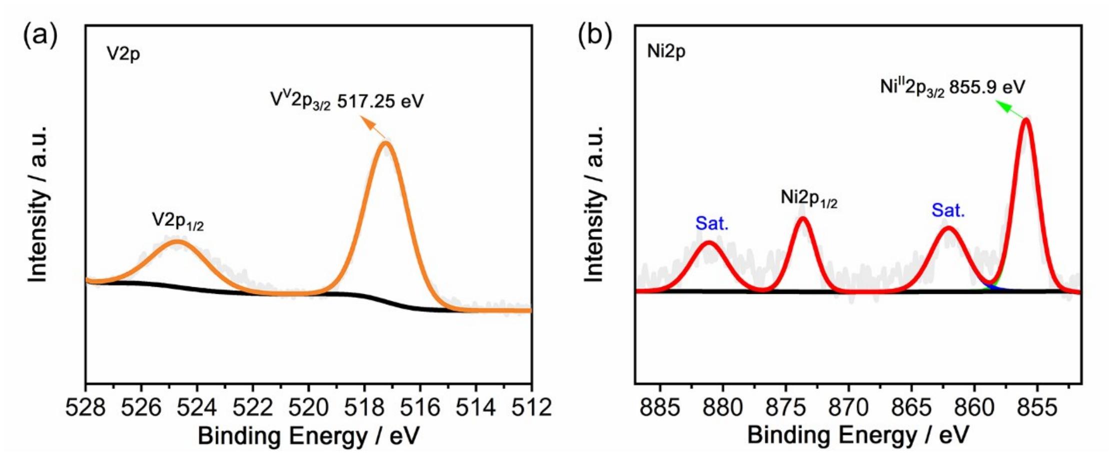

Figure S4. XPS spectra of V (a) and Ni (b) in **V-Ni-MOF**.

6. TGA curve of V-Ni-MOF

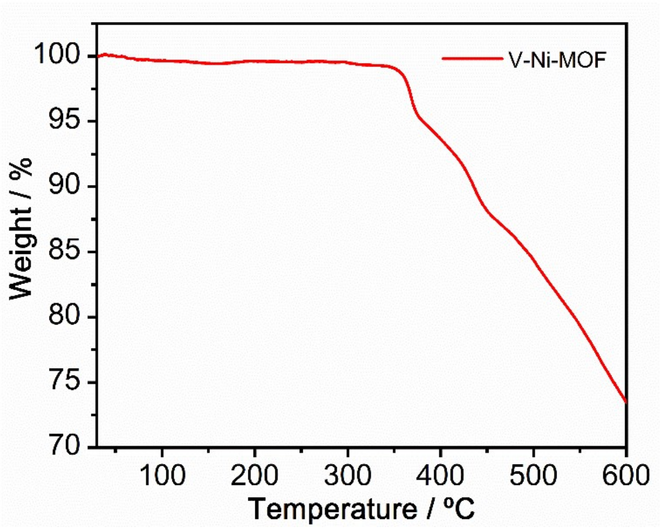

Figure S5. The TGA curve of **V-Ni-MOF**.

7. PXRD patterns of V-Ni-MOF after immersing in various solvents

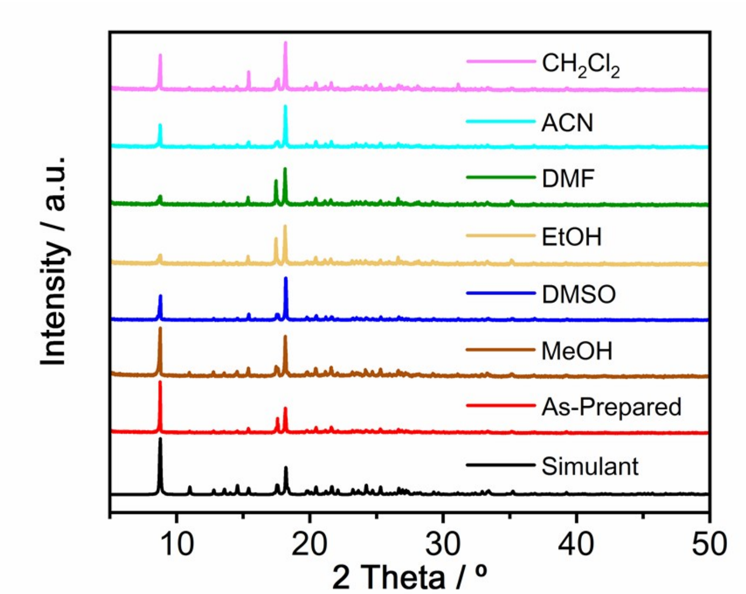

Figure S6. The PXRD patterns of **V-Ni-MOF** after immersing in various solvents for 7 days.

8. [1]H-NMR Spectra of the sulfides

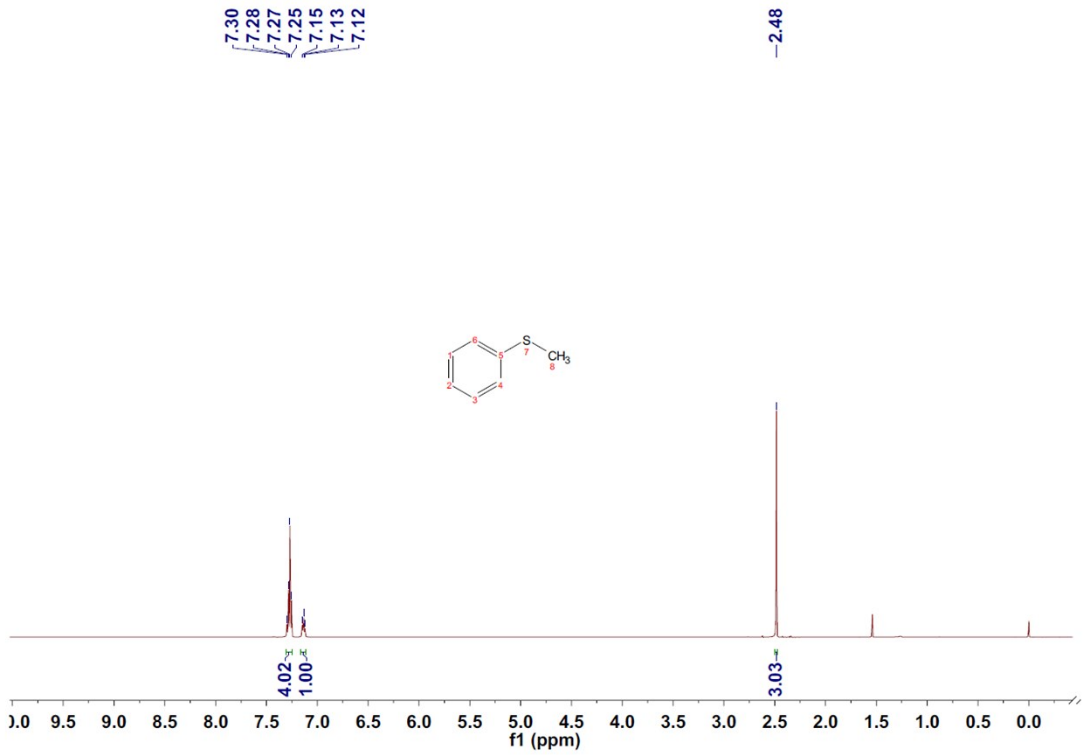

^{1}H-NMR Spectra of methyl phenyl sulfide.

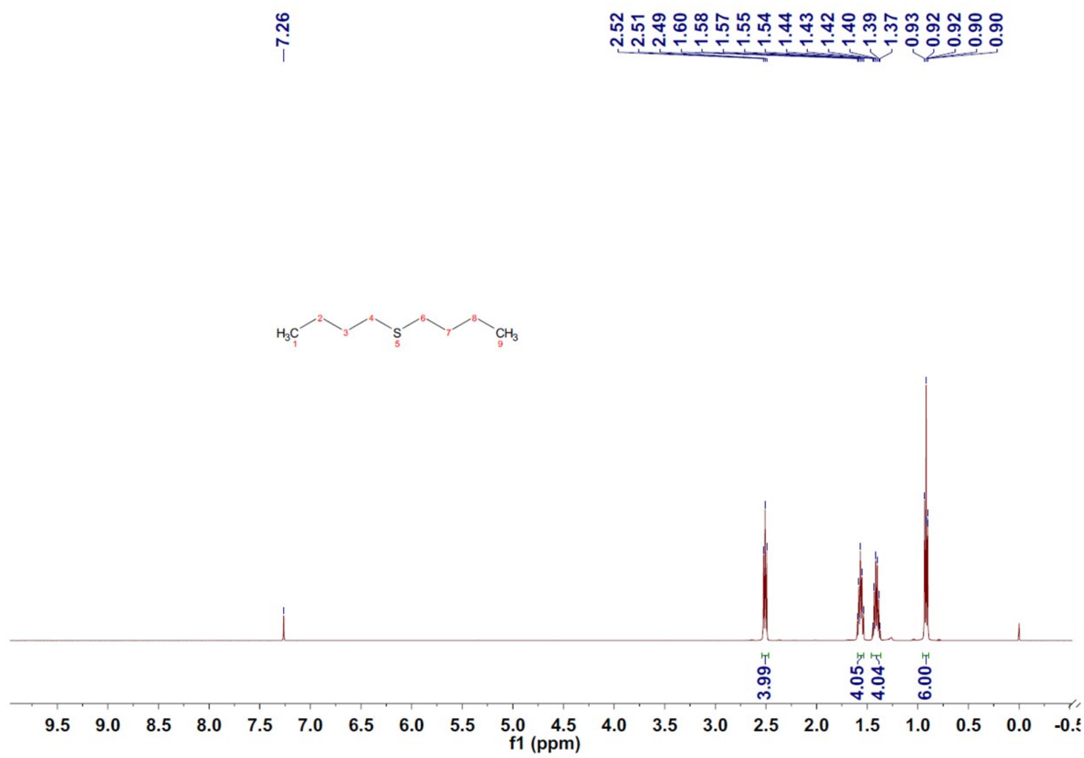

^{1}H-NMR Spectra of dibutyl sulfide.

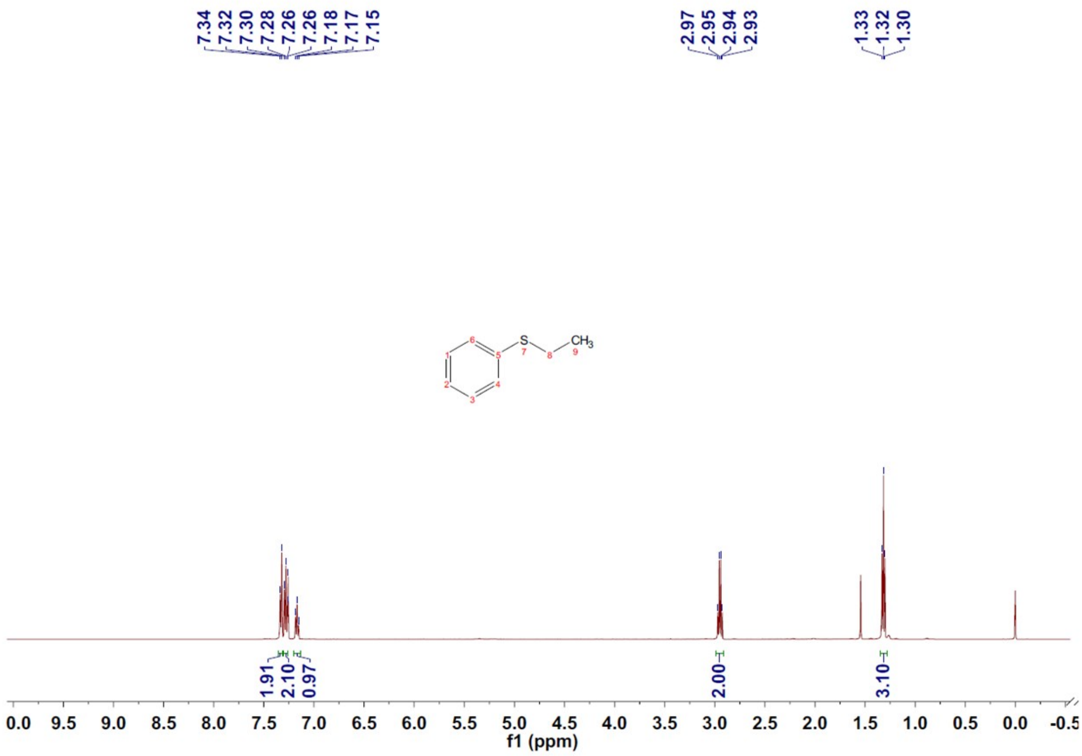

[1]H-NMR Spectra of ethyl phenyl sulfide.

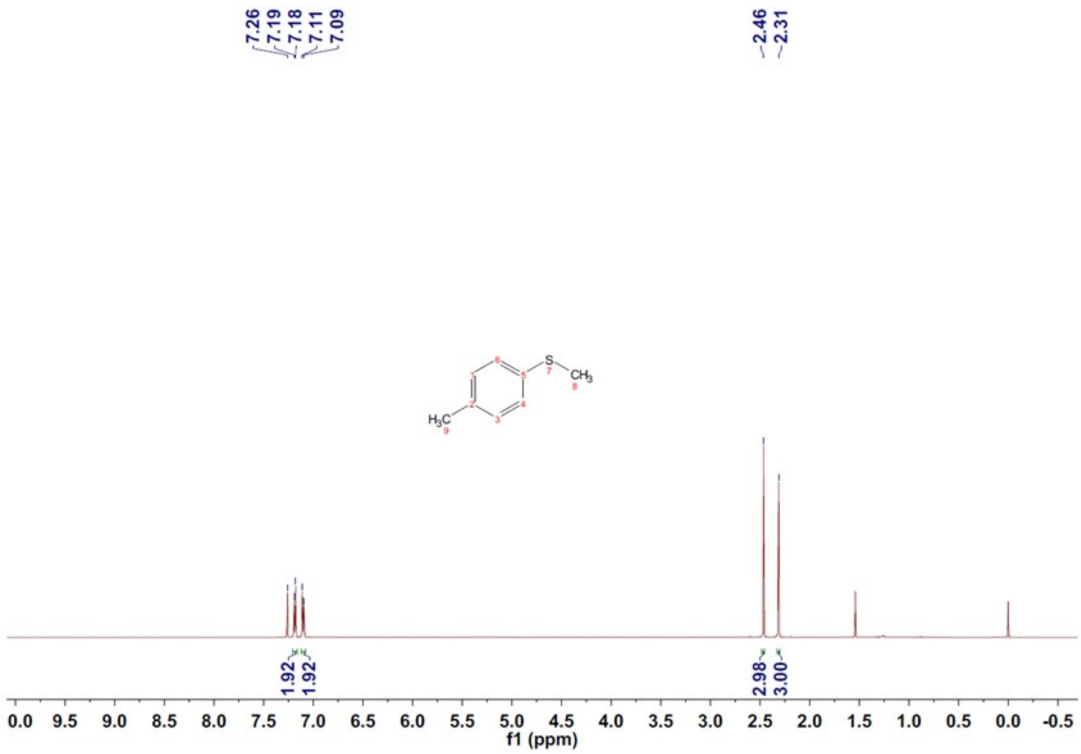

[1]H-NMR Spectra of methyl p-tolyl sulfide.

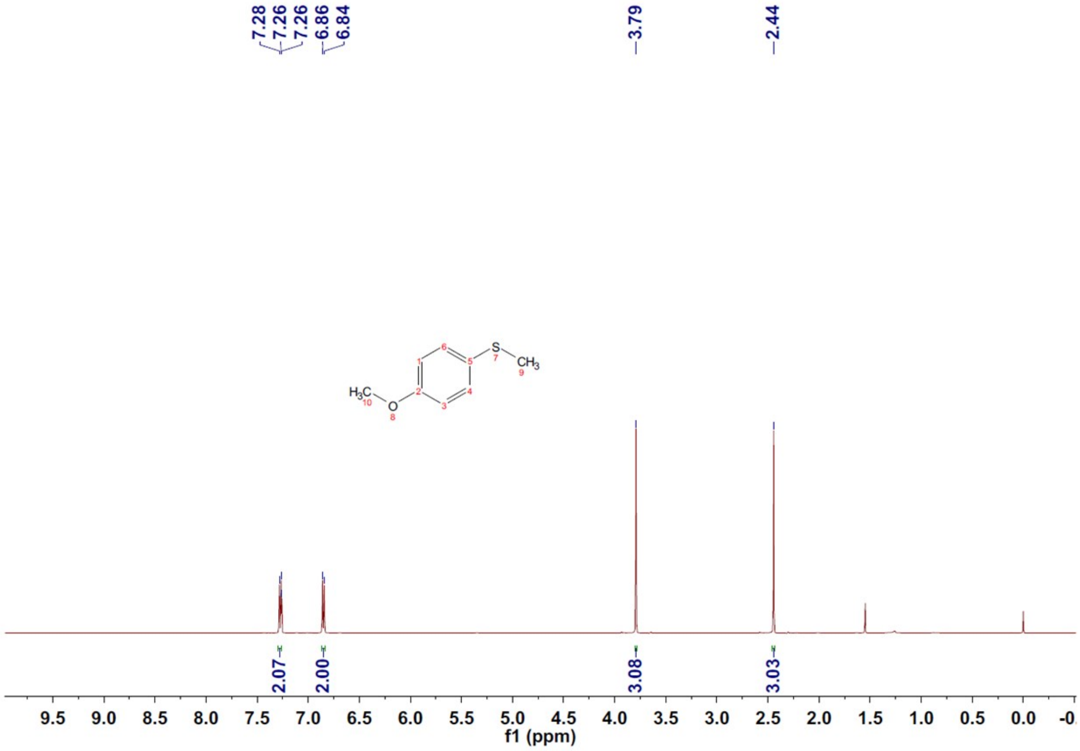

[1]H-NMR Spectra of 4-methoxythioanisole.

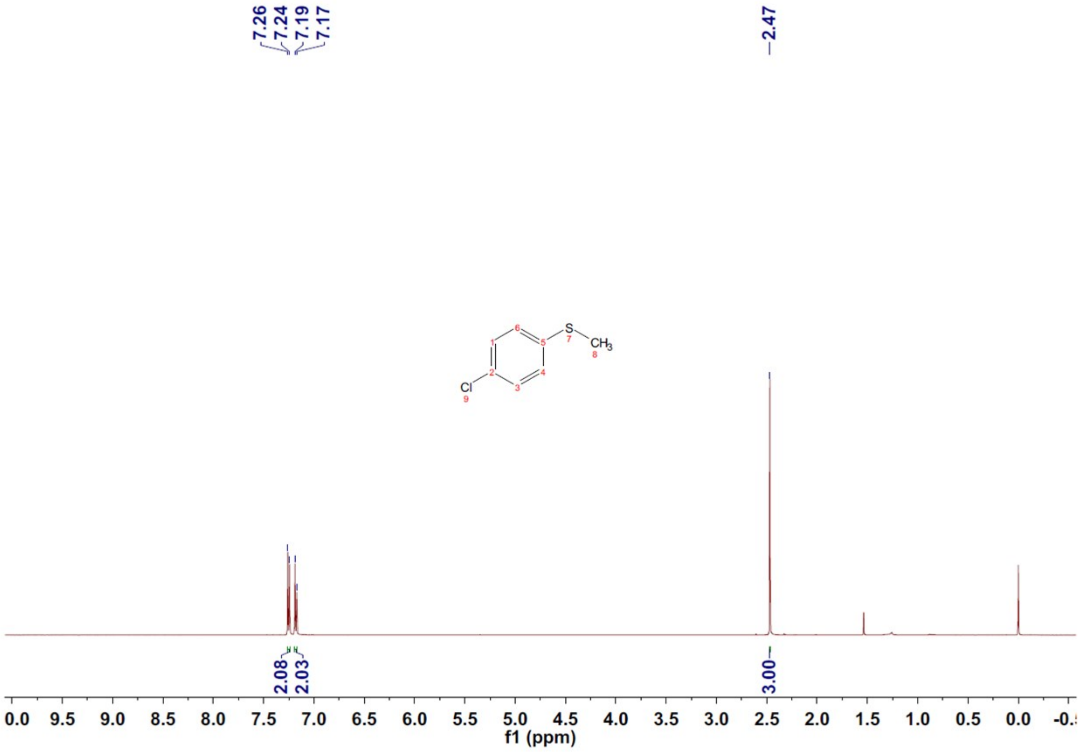

[1]H-NMR Spectra of 4-chlorothioanisole.

9. [1]H-NMR Spectra of the sulfones

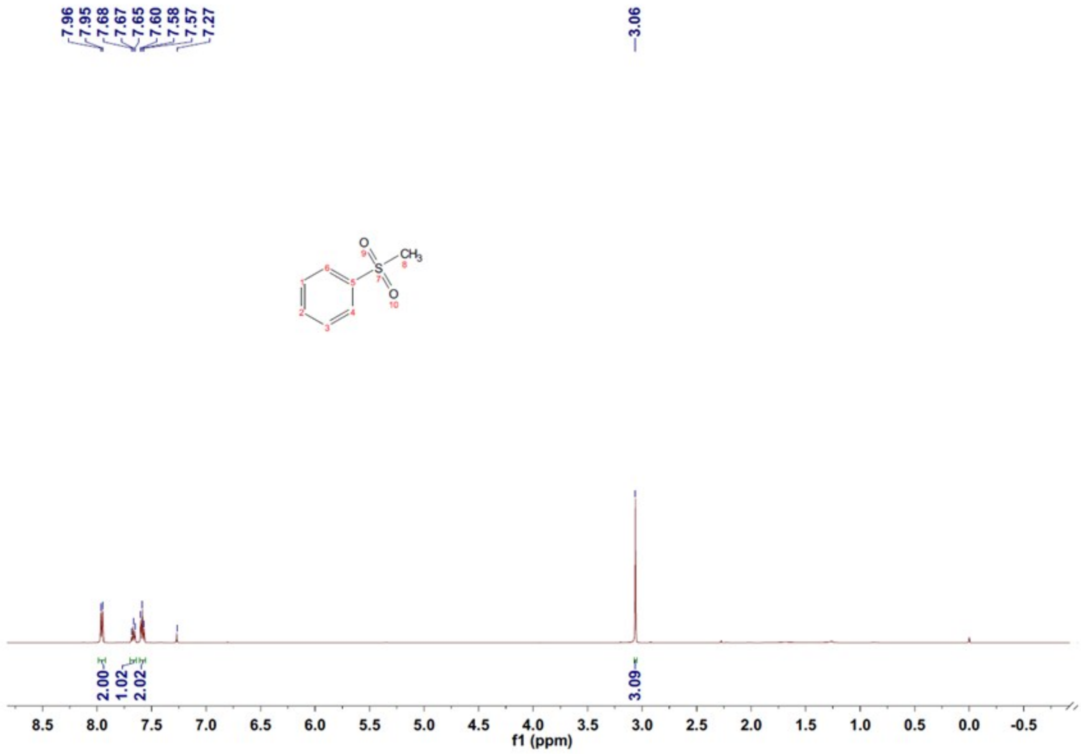

[1]H-NMR Spectra of methyl phenyl sulfone.

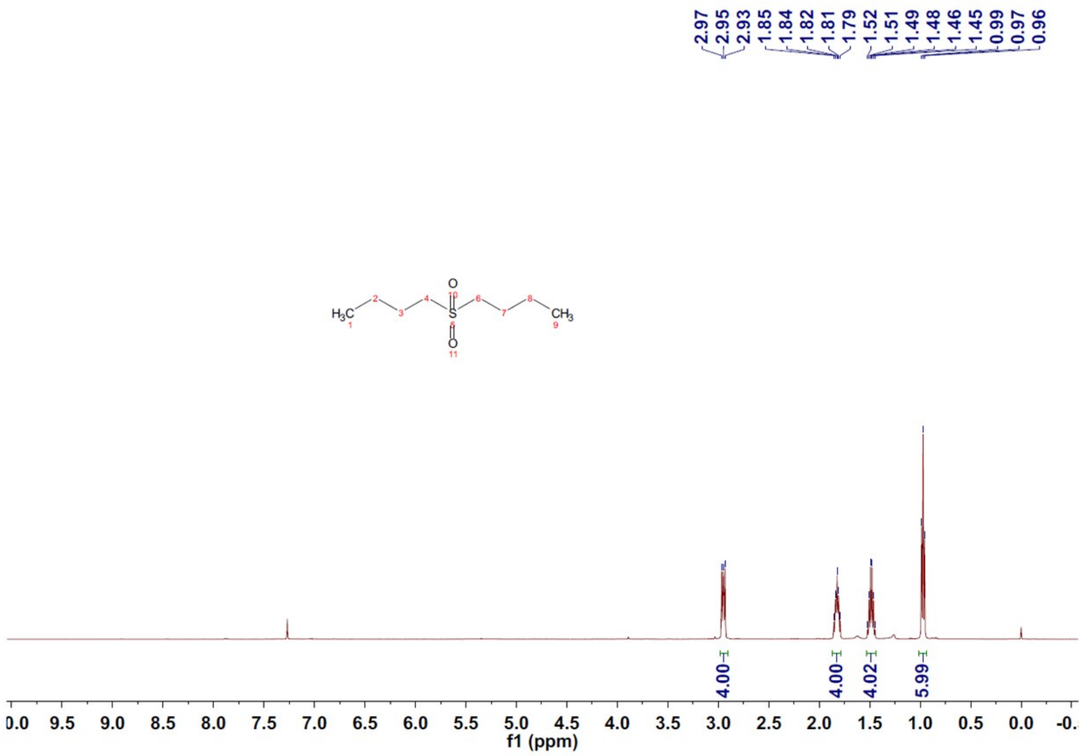

[1]H-NMR Spectra of dibutyl sulfone.

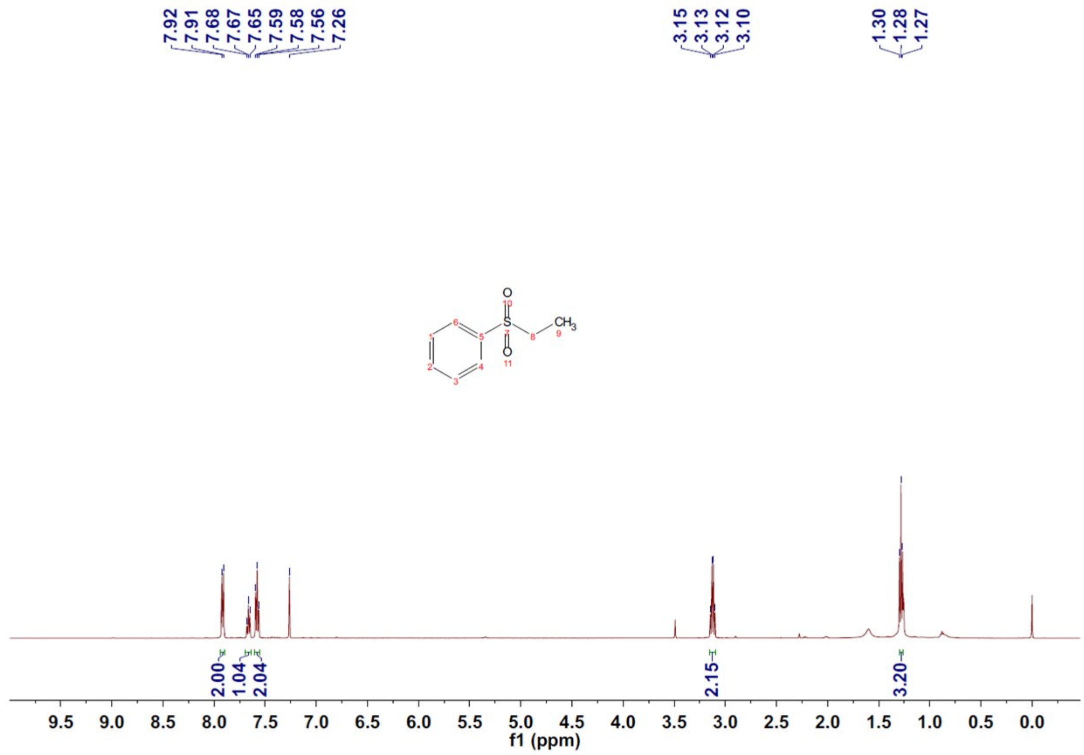

[1]H-NMR Spectra of ethyl phenyl sulfone.

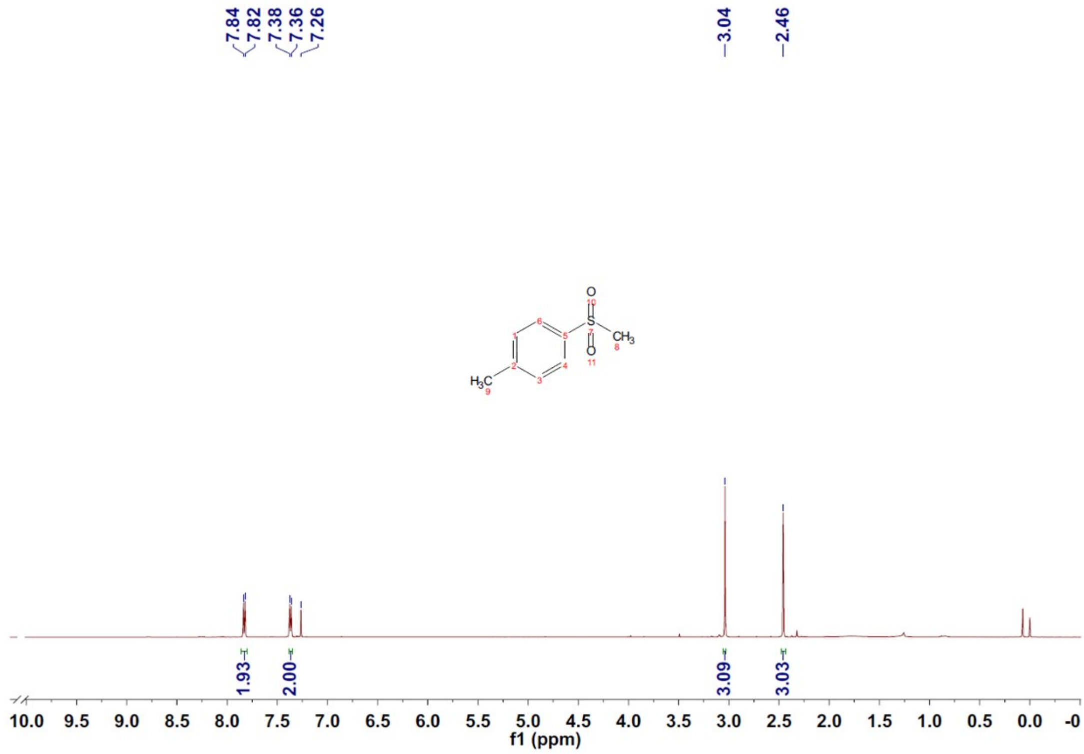

[1]H-NMR Spectra of methyl p-tolyl sulfone.

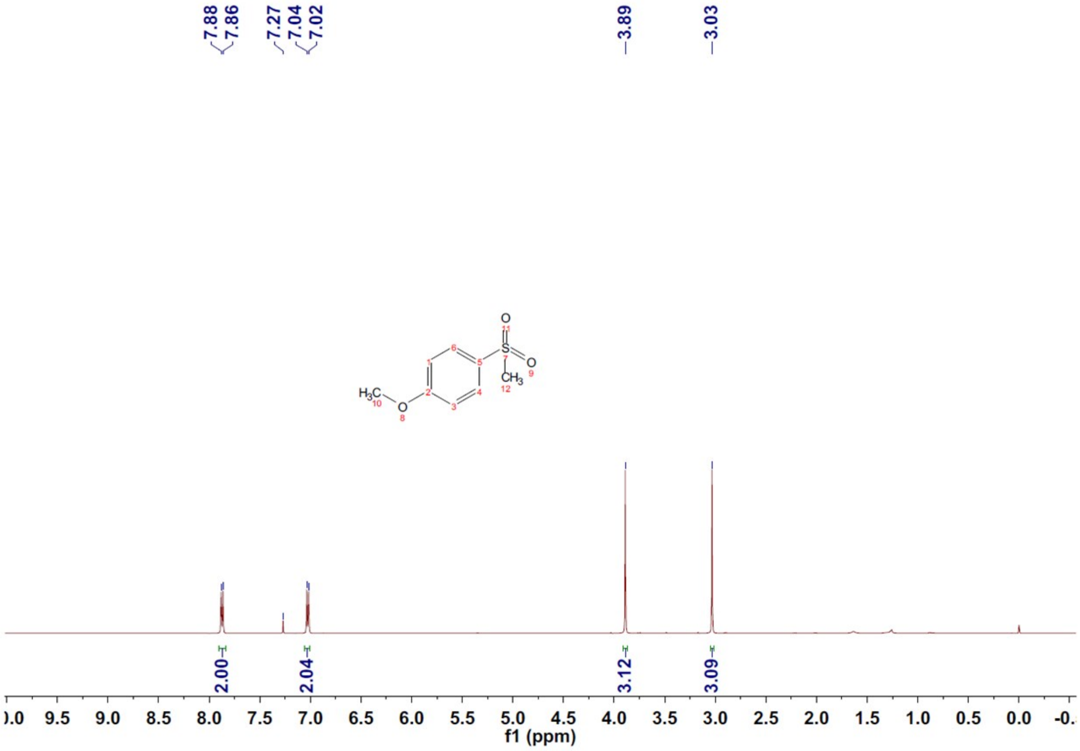

[1]H-NMR Spectra of 4-methoxyphenylmethylsulfone.

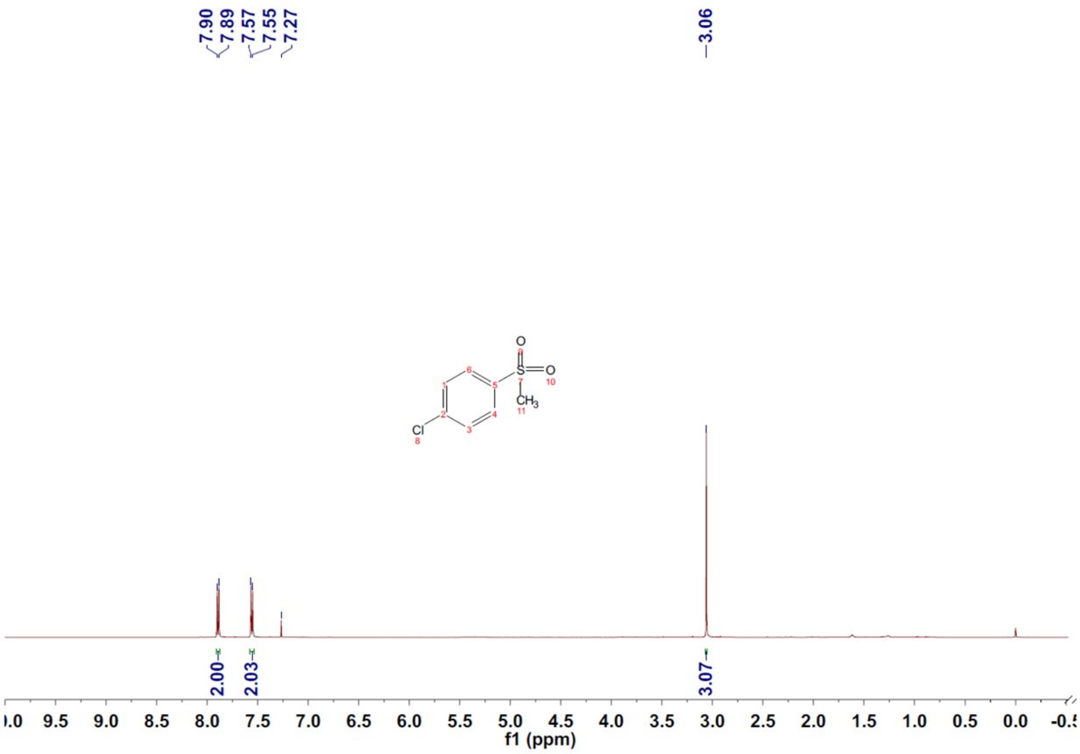

[1]H-NMR Spectra of 4-chlorophenyl methyl sulfone.

10. Recycling tests of the V-Ni-MOF

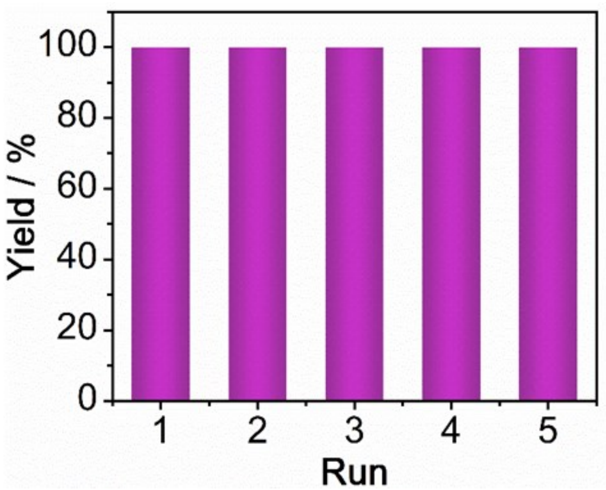

Figure S7. Recycling tests for sulfide oxidation using the **V-Ni-MOF**.

11. SEM images of V-Ni-MOF

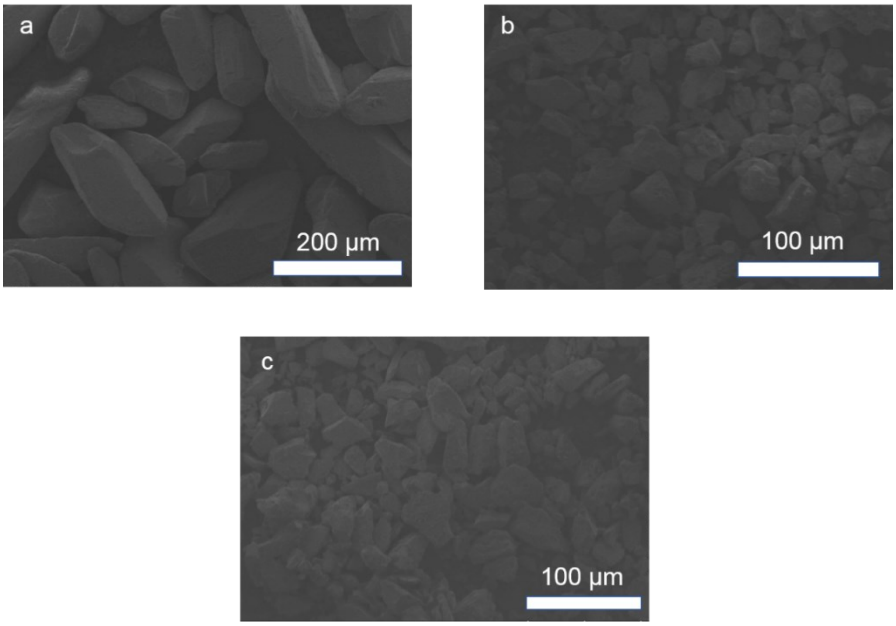

Figure S8. (a) The crystal SEM images of **V-Ni-MOF**; (b) SEM images of the grinded **V-Ni-MOF**; (c) SEM images of the grinded **V-Ni-MOF** after sulfide oxidation.

12. Compared with the crystalline materials containing polyoxovanadate

Table S3. Compared with the crystalline materials containing polyoxovanadate used in oxidation reactions of sulfides

Entry	Catalyst	Time (h)	Oxidant	T (°C)	Con. (%)	Reference
1	$K_6H[V^V{}_{17}V^{IV}{}_{12}(OH)_4O_{60}(OOC(CH_2)_4COO)_8]\cdot nH_2O$	1	TBHP	25	98	1
2	$[(C_2N_2H_8)_4(CH_3O)_4V^{IV}{}_4V^V{}_4O_{16}]\cdot 4CH_3OH$	4	TBHP	40	100%	2
3	$[Co_2L_{0.5}V_4O_{12}]\cdot 3DMF\cdot 5H_2O$	4	TBHP	50	> 99%	3
4	$[V_8{}^{IV}O_8(CH_3O)_{16}(C_2O_4)](C_6NH_{16})_2(CH_3OH)_2$	4	TBHP	40	100%	4
5	$(NH_2Me_2)_{12}[(V_5O_9Cl)_6(L)_8]\cdot[MeOH]_7$	1	TBHP	25	100%	5
6	$[Co_2L_{0.5}V_4O_{12}]\cdot 3DMF\cdot 5H_2O$	4	H_2O_2	50	trace	3
7	V-Ni-MOF	0.75	TBHP	25	100%	This work
8	V-Ni-MOF	0.25	TBHP	40	100%	This work
9	V-Ni-MOF	1	H_2O_2	40	100%	This work

13. References

1. K. Wang, Y. Niu, D. Zhao, Y. Zhao, P. Ma, D. Zhang, J. Wang and J. Niu, The Polyoxovanadate-Based Carboxylate Derivative $K_6H[V^V{}_{17}V^{IV}{}_{12}(OH)_4O_{60}(OOC(CH_2)_4COO)_8]\cdot nH_2O$: Synthesis, Crystal Structure, and Catalysis for Oxidation of Sulfides, *Inorg. Chem.*, 2017, **56**, 14053-14059.
2. J. P. Cao, Y. S. Xue, N. F. Li, J. J. Gong, R. K. Kang and Y. Xu, Lewis Acid Dominant Windmill-Shaped V_8 Clusters: A Bifunctional Heterogeneous Catalyst for CO_2 Cycloaddition and Oxidation of Sulfides, *J. Am. Chem. Soc.*, 2019, **141**, 19487-19497.
3. B. B. Lu, J. Yang, Y. Y. Liu and J. F. Ma, A Polyoxovanadate–Resorcin[4]arene-Based Porous Metal–Organic Framework as an Efficient Multifunctional Catalyst for the Cycloaddition of CO_2 with Epoxides and the Selective Oxidation of Sulfides, *Inorg. Chem.*, 2017, **56**, 11710-11720.
4. Q. D. Ping, J. P. Cao, Y. M. Han, M. X. Yang, Y. L. Hong, J. N. Li, J. L. Wang, J. L. Chen, H. Mei and Y. Xu, Eight-membered ring petal-shaped V_8 cluster: An efficient heterogeneous catalyst for selective sulfur oxidation, *Inorg. Chim. Acta*, 2021, **517,** 120198.
5. H. M. Gan, C. Qin, L. Zhao, C. Sun, X. L. Wang and Z. M. Su, Self-Assembled Polyoxometalate-Based Metal-Organic Polyhedra as an Effective

Heterogeneous Catalyst for Oxidation of Sulfide, *Cryst. Growth Des*, 2021, **21**, 1028-1034.